PROGRESSIVE COLLAPSE ANALYSIS THROUGH STRENGTH DEGRADATION AND FRACTURE IN THE MIXED LAGRANGIAN FRAMEWORK

O. Lavan[1], M.V. Sivaselvan[2], A.M. Reinhorn[3] and G.F. Dargush[4]

[1] *Senior Lecturer, Faculty of Civil and Environmental Engineering, Technion Israel Institute of Technology, Haifa, Israel*

[2] *Assistant Professor, Dept. of Civil, Environmental and Architectural Engineering, University of Colorado at Boulder, Boulder, CO, USA*

[3] *Professor, Dept. of Civil, Structural and Environmental Engineering, University at Buffalo, Buffalo, NY, USA*

[4] *Professor, Dept. of Mechanical and Aerospace Engineering, University at Buffalo, Buffalo, NY, USA*

Email: lavan@tx.technion.ac.il, siva@colorado.edu, Reinhorn@buffalo.edu, gdargush@eng.buffalo.edu

ABSTRACT:
Dynamic progressive collapse analysis faces a great number of obstacles that often lead to the collapse of the analysis prior to the actual analysis of collapse. Hence, it is argued here that a robust analysis framework should be adopted and modified to account for the different stages of collapse. The Mixed Lagrangian Formulation (MLF) that was shown to be very robust and to scale very well to large scale problems was, thus, adopted as a framework to accommodate such analysis. This approach allows the analysis of structures in the elastic and in the plastic range while automatically considering geometric nonlinearity. It is hence natural to extend its capabilities to account for strength degradation and fracture, which is the purpose of this paper.

KEYWORDS:
Progressive collapse, Mixed Lagrangian Formulation, Fracture, Strength degradation

1. INTRODUCTION

The earthquake engineering community has tried to avoid the use of complex analyses for the purpose of design. The analysis adopted thus usually makes use of static tools or modal spectral analysis that is modified to approximate the nonlinear response of buildings. This approach has several limitations. First, the approximate analysis might not lead to satisfactory approximations. The severity of this problem is expected to increase as the structure is closer to collapse and its behavior becomes more complex. Second, suppose a building was indeed designed not to collapse during a given level of earthquakes. Its capacity to sustain stronger earthquakes would remain unknown, that is to say, its response to stronger earthquakes is unidentified. This is problematic because new approaches for the design of buildings could, perhaps, increase their capacity to withstand stronger earthquakes than expected, without a significant increase in their cost. Finally, without a valid analysis tool that is capable to predict the seismic behavior of buildings up to collapse, the capacity of existing buildings remains unknown, and decisions on the need, level and design of their retrofit remains subjective. For those reasons one can conclude that there is no escape from developing an advanced analysis tool to address the issue of progressive collapse prediction.

In the sequence of progressive collapse, the structure, or parts of the structure, go through different stages. Some parts of the structure can be assumed to be linear elastic at some stages. At a later stage some parts might yield and go into the plastic range. As the deformations grow, stiffness and strength degradation may take place, as well as possible buckling, and other geometric nonlinear phenomena. Subsequently, sudden strength loss or fractures are expected, leading to redistribution of the loads, as well as introducing step forces to the structure. As regions in the structure loose their strength, they might be detached from the structure. At the final stage of collapse, these detached parts of the structure, or other objects which were not attached to the structure to begin with (such as live loads), might hit other parts of the structure and introduce additional impulses or step forces. The different phenomena described above pose large difficulties for the analysis.

The abovementioned obstacles present in dynamic progressive collapse analysis often lead to the collapse of the analysis prior to the actual analysis of collapse. Hence, it is argued here that a robust analysis framework should be adopted and modified to account for the different stages of collapse. The Mixed Lagrangian Formulation (MLF) (Sivaselvan and Reinhorn, 2006) that was shown to be very robust and to scale very well to large scale problems (see Reinhorn *et al*., 2007) was, thus, adopted. This approach allows the analysis of structures in the elastic and in the plastic range, while automatically considering geometric nonlinearity. It is hence natural to extend its capabilities to account for strength degradation and fracture, which is the purpose of the present paper. An additional motivation for extending MLF to account for fracture is the fact that in cases where fracture is considered, traditional structural analysis approaches usually take a negative stiffness into account. This requires special treatment and solution methods, such as the arc length method (*e.g.*, Crisfield, 1991), as well as very small time steps, and often lead to instability of the analysis. Since MLF uses the forces as the main variables rather than the displacements, it retains the robustness that was observed in the plastic analysis. Another advantage of MLF in that context is that it makes use of the weak form of the problem over time. Hence, in problems where sudden changes are expected in the response of structures, a stable behavior is observed.

2. OVERVIEW OF MLF

The MLF was introduced by Sivaselvan and Reinhorn (2006) for the dynamic analysis of elastic-plastic systems. It consists of a set of equilibrium equations in the direction of the degrees of freedom, and a set of equations for compatibility of velocities in the direction of the impulses of internal forces. These equations, which were attained by formulating appropriate Lagrangian and dissipation functions and substitution to the Euler-Lagrange equations, have the following form:

$$\begin{aligned} \mathbf{M}\dot{\mathbf{v}} + \mathbf{C}\mathbf{v} + \mathbf{B}\mathbf{F} &= \mathbf{P} \\ \mathbf{A}\dot{\mathbf{F}} + \frac{\partial \varphi(\mathbf{F})}{\partial \mathbf{F}} - \mathbf{B}^T\mathbf{v} &= \mathbf{0} \end{aligned} \tag{2.1}$$

where $\mathbf{v}$=vector of velocities of the degrees of freedom; $\mathbf{F}$=vector of internal forces; $\mathbf{M}$ =mass matrix; $\mathbf{C}$ =damping matrix; $\mathbf{B}$ =equilibrium matrix that transforms the internal forces $\mathbf{F}$ into equivalent nodal forces; $\mathbf{P}$=vector of external nodal forces; $\mathbf{A}$=flexibility matrix; $\varphi(\mathbf{F})$=dissipation function due to plasticity; $\mathbf{0}$=a zero vector; t = time; a dot represents a derivative with respect to time and the superscript T represents the transpose of a matrix.

The left hand side of the first of these equations is comprised of the inertia forces, the damping forces and the internal forces, respectively, while the right hand side has the external forces. In the second of these equations the first term on the left hand side is the rate of the elastic part of the displacements in the direction of the internal forces, the second term is the rate of the plastic displacement and the third is the total rate of displacement in this direction. Thus, the first set represents dynamic equilibrium, while the second set constitutes compatibility of velocities. It has been shown (Sivaselvan and Reinhorn, 2006) that these equations also hold when the matrix $\mathbf{B}$ is a function of the coordinates, $\mathbf{u}$, *i.e.* when geometric nonlinearity is considered.

The MLF was introduced for a general case in which the mass and damping matrices may be singular. For the purpose of providing a sketch of the derivation of the MLF, the mass matrix will be assumed nonsingular. Equations 2.1 are first discretized at time i+½ by using the central difference approach. The velocities at time n+1, $\mathbf{v}_{n+1}$, are then isolated from the discretized version of the first of Eqn. 2.1 and substituted to the second of Eqn. 2.1 to result in the following equation for $\mathbf{F}_{n+1}$:

$$\bar{\mathbf{A}}\mathbf{F}_{n+1} + \frac{1}{2}\frac{\partial \varphi}{\partial \mathbf{F}}\bigg|_{n+1} + \bar{\mathbf{b}} = \mathbf{0} \tag{2.2}$$

where the $\bar{\mathbf{A}}$ matrix and $\bar{\mathbf{b}}$ vector are known at the time step of computation. Following the derivation by

Sivaselvan and Reinhorn (2006), one can integrate Eqn. 2.2 with respect to $\mathbf{F}_{n+1}$ to obtain the following optimization problem for the time step n:

$$\begin{aligned} \min \quad & \frac{1}{2}\mathbf{F}_{n+1}^T\bar{\mathbf{A}}\mathbf{F}_{n+1} + \bar{\mathbf{b}}^T\mathbf{F}_{n+1} \\ \text{s.t.} \quad & \frac{1}{2}\varphi\left(\mathbf{F}_{n+1}\right) \le 0 \end{aligned} \tag{2.3}$$

3. STRENGTH DEGRADATION AND FRACTURE IN MLF

In the derivations to follow we modify the dissipation function and the numerical scheme, and extend the capabilities of MLF to account for strength degradation and fracture through "shrinking" the yield surface. Some insight to the MLF behavior in the case of fracture is introduced as well. For the sake of simplicity the main idea of "shrinking" the yield surface is demonstrated by using a simple case of "one-dimensional" plasticity of a single spring element. The methodology, however, has been successfully applied to the case of multidimensional plasticity.

3.1. "Shrinking" the yield surface

In the case of an elastic perfectly plastic element, the function $\varphi(\mathbf{F})$ takes the form:

$$\varphi\left(\mathbf{F}\right) = \begin{cases} 0 & \text{if elastic, } i.e., \ f\left(\mathbf{F}\right) < 0 \\ \infty & \text{if plastic, } i.e., \ f\left(\mathbf{F}\right) \ge 0 \end{cases} \tag{3.1}$$

where f can be thought of as the loading function of the member or the plastic hinge. This representation in MLF actually constrains the force vector, **F**, to be in the feasible region (elastic or plastic). This concept, as well as the concept of "shrinking" the loading function, could be easily illustrated by using a single one dimensional element model. Here, the function f is simply $f(F)=|F|-F_y$, where F_y is the yield level of this force. The dissipation function is, thus, zero in the elastic range, *i.e.* when $f(F)=|F|-F_y<0$ and becomes infinite when $f(F)=|F|-F_y=0$. The case where $f(F)=|F|-F_y>0$ is actually infeasible and cannot be reached.

Shrinking the yield surface in this case could be easily obtained by reducing the value of F_y. In this case the upper bound on F that results from the constraint in the optimization problem of Eqn. 2.3 and the dissipation function, is reduced, and strength reduction is achieved. For the function f presented earlier, the change of strength is isotropic. Different rules, however, can be adopted by modifying this function. The function $f(F)=(F-F_y^{(-)})(F-F_y^{(+)})$ for example, could result in an anisotropic rule by changing $F_y^{(-)}$ and $F_y^{(+)}$ according to different criteria and, of course, similar techniques could be applied to the multidimensional case.

3.2. Strength degradation versus fracture

Before starting with the derivations it is important to distinguish strength degradation from fracture. Although both phenomena involve reduction of strength, while strength degradation does not involve sudden changes in the actual force, fracture does (see Fig. 1). Hence, computationally speaking, fracture is a more complex problem both to model and to solve. These large changes in the actual force often make the computational scheme unstable. However, since the main variables used by MLF are forces and not displacements, fracture is associated with changing the constraints on the forces rather than using a "negative stiffness." Hence, MLF is expected to be stable even when fracture occurs.

In the case of strength degradation, as presented by Fig. 1a, the modeling and implementation in the MLF framework is straightforward. Since the degradation in this case is dictated by the *history* of the state variables only, but not on their current values, the dissipation function could evolve in each time step based on the past behavior of the structure. Moreover, sudden changes in the actual force are not expected. Hence, in each time step, the only change from the traditional MLF is the fact that the dissipation function should be updated. The structure

of the dissipation function and its dependency on the states at the time $n+1$, however, remains with no change. It should be noted that the conventional displacement based analysis usually has no computational difficulty in this case as well.

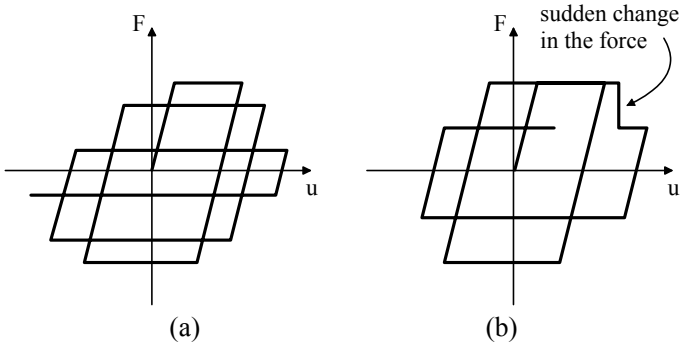

Figure 1 Hysteretic loops with (a) strength degradation and (b) fracture

As opposed to the case of strength degradation, in the case of fracture, the dissipation function depends also on *current* values of the state variables. Hence, the structure of this function and its dependency on the states at the time $n+1$, might change. Since forces are the main variables in MLF, these changes may require some modifications. For example, in the one dimensional plasticity case presented earlier, the variation of F_y could depend on the maximum displacement experienced by the element up to the current time. This maximum displacement itself depends on the displacement at the end of the current time step. This displacement is yet unknown and, moreover, is not a variable. Hence, when the dependency involves displacements or energies, modifications are required. In addition, the sudden change in the actual force will require some small modifications to the numerical scheme. It should be noted that the displacement based analyses tend to become unstable when fracture is involved, even when sophisticated and computationally expensive analysis tools are applied. The modifications to MLF proposed here, on the other hand, lead to a very stable scheme, as will be shown subsequently, with a negligible addition of computational effort.

3.3. Why is MLF so robust in fracture?

As will be shown by the examples, the MLF scheme is very robust in terms of time step size and stability, even when sudden fracture is considered. In this section some insight to the reason for the enhanced robustness is presented. In MLF, the main variables used are *forces* and not displacements, and fracture is associated with *changing the constraints* on the forces rather than using a "negative stiffness". Hence, in each time step the forces are actually attained by solving a constrained optimization problem whose solution is bounded to be in the elastic or in the plastic regions. Since the feasible region of the force vector is a closed region, the force vector can not go beyond the plastic region and hence does not become unstable. This approach is illustrated in Fig. 2 where the optimization problem for a case of a single unidirectional member is shown.

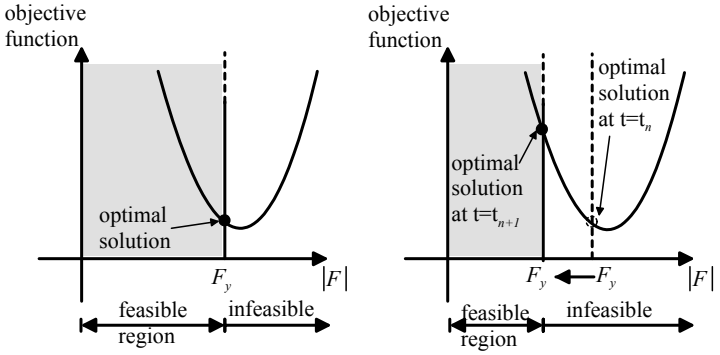

Figure 2 Optimization problem for a one dimensional plasticity model (a) before strength reduction and (b) changing during strength reduction

Figure 2a shows the objective function (parabola), the constraint ($|F|$-$F_y \leq 0$), the feasible region (in gray) and the optimal solution (dot), right before fracture. Figure 2b presents a similar illustration at the time of fracture. As can be seen, "shrinking" the yield surface is associated here with reducing the value of F_y, hence, reducing the upper bound on the actual value of F. This results in a drop in the actual force that is actually attained by solving an optimization problem.

4. NUMERICAL SCHEME

As an example, the rule considered for fracture is presented in Fig. 3a, where $\bar{u}^{(i)}_{\max}$ represents the maximum displacement ever experienced by the member/plastic hinge up to the current point in time.

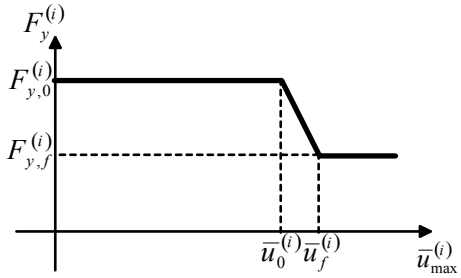

Figure 3 Description of strength function

Here F_y depends upon $\bar{u}^{(i)}_{n+1}$, the maximum displacement ever experienced by the member/plastic hinge i at time $n+1$, while the variables used in Eqn. 2.3 are forces. Consequently, F_y is first reformulated in terms of $\bar{u}^{(i)}_{n+1}$, which is then evaluated as a function of $\mathbf{F}_{n+1}$ so that the final result would be $F_y(\mathbf{F}_{n+1})$.

4.1. Some numerical insight

In order to understand the numerical issues related to fracture it would be beneficial to first gain some insight to the behavior of the problem through the temporally continuous Eqn. 2.1. For the sake of discussion, let us first look at a massless spring under a displacement controlled loading with a very slow rate of displacement. Since the mass and damping are zero, and the rate of displacement is very small, and Eqn. 2.2 takes the form:

$$A\dot{F} + \frac{\partial \varphi}{\partial F} = 0 \tag{4.1}$$

Equation 4.1 shows that when the internal force drops and $\dot{F}$ shows a negative δ (Dirac) function, in order to satisfy the compatibility equation, $\partial\varphi / \partial F$ should have a positive δ function. This type of behavior could be generalized to other types of loading and is qualitatively illustrated in Fig. 4a.

4.2. Numerical behavior

A qualitative behavior of the numerical solution for the same system employed for Fig. 4a, using the traditional numerical scheme of MLF with the modified loading function, is presented in Fig. 4b. As can be seen, the drop in the internal force in the time step where fracture occurs (from t_n to t_{n+1}) seems precise. However, the drop in the force seems to somewhat "overshoot" in the time step following the fracture. In order to understand the reason for that it is interesting to explore the behavior of $\partial\varphi / \partial F$ in the discretized solution, which is also presented in Fig. 4b. When fracture occurs, the value of $\partial\varphi / \partial F$ has to have a "jump" to account for the δ seen in the continuous behavior. This can also be seen from the discretized compatibility equation (discretized version of the second of Eqn. 2.1). Here, a large (negative) difference, F_{n+1}-F_n, and a small time step, h, lead to a large value of $\partial\varphi / \partial F\,|_{n+1}$. For the following time step, the discretized compatibility equation takes the form

$$\mathbf{A}\left(\frac{\mathbf{F}_{n+2} - \mathbf{F}_{n+1}}{h}\right) + \frac{1}{2}\left(\left.\frac{\partial \varphi}{\partial \mathbf{F}}\right|_{n+2} + \left.\frac{\partial \varphi}{\partial \mathbf{F}}\right|_{n+1}\right) - \mathbf{B}^T\left(\frac{\mathbf{v}_{n+2} + \mathbf{v}_{n+1}}{2}\right) = \mathbf{0} \tag{4.2}$$

In order to satisfy this equation with the large value of $\partial\varphi / \partial F|_{n+1}$ dictated from the previous step, the value of $\partial\varphi / \partial F|_{n+2}$ has to have a very small value and, probably, should change its sign. This parameter is, however, restricted in sign since: (a) it is actually the plastic rate of deformation that physically cannot be in an opposite direction to the force, and (b) it is actually the Lagrange multiplier in the optimization problem. This variable, hence, takes the value of zero which: (a) implies an elastic state, and (b) enforces an additional (negative) difference, F_{n+2}-F_{n+1}, so as to satisfy the compatibility Eqn. 4.2. This additional difference in forces is actually the overshoot seen in the solution of Fig. 4b.

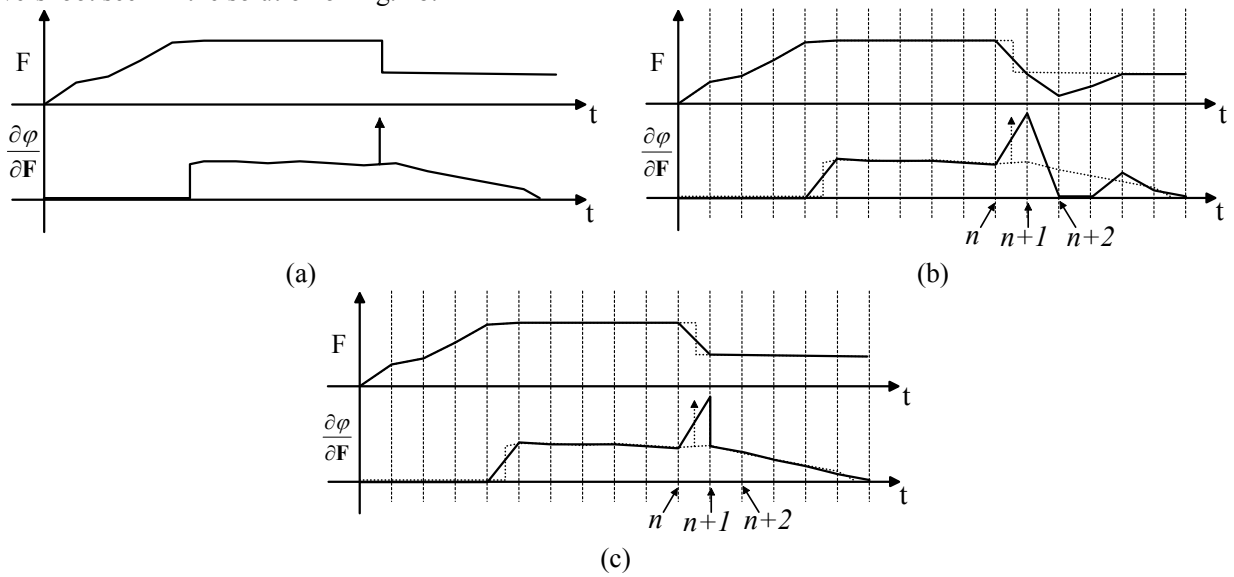

Figure 4 Qualitative illustration of the behavior of a spring during fracture: (a) analytical, (b) numerical (continuous line) versus analytical (dotted line), and (c) modified numerical (continuous line) versus analytical

4.3. Numerical modifications

It is argued here that the value computed for $\partial\varphi / \partial F|_{n+1}$ is reasonable and that it takes into account the δ experienced during the time step in an integral sense. However, this value is not appropriate for use in the next time step, where the δ should have no effect. Hence, it is proposed here to use two values for $\partial\varphi / \partial F|_{n+1}$; one for the previous time step and one for the following time step, as illustrated in Figure 4c. The evaluation of $\partial\varphi / \partial F|_{n+1}$ to be used in the time step following the fracture relies on the compatibility equation at the time t_{n+1} and some insight from the theory of plasticity. This is actually an important part of the work that cannot be discussed here due to space limitations.

5. EXAMPLE

A two story shear frame is chosen to demonstrate the behavior of the problem and the numerical solution. In the global DOFs, the mass matrix is a 2×2 identity matrix (*i.e.*, $m_1 = m_2 = 1$), while the damping matrix is a 2×2 zero matrix. The flexibility matrix in the forces coordinate system and the equilibrium matrix are given by

$$\mathbf{A} = \frac{1}{2 \cdot 4\pi^2}\begin{bmatrix} 1 & 0 \\ 0 & 1 \end{bmatrix} \quad ; \quad \mathbf{B} = \begin{bmatrix} 1 & -1 \\ 0 & 1 \end{bmatrix} \tag{5.1}$$

The external force vector is taken as $\mathbf{P} = -\mathbf{M1}a_g(t)$, where $\mathbf{1}$ is a unit vector of appropriate size and $a_g(t)$ is the ground acceleration that is taken here as the LA02 record. This record is actually the Imperial Valley, 1940, El Centro earthquake scaled by a factor of 2.01 (Somerville *et al.*, 1996). The model of Fig. 3 was used to describe the variation of the yield force and the initial and the minimum yield force vectors are $\mathbf{F}_{y,0} = [3/4 \quad 3/4]^T$ and

$\mathbf{F}_{y,f} = [3/8 \quad 3/8]^T$, respectively. The transition from the initial yield force to the minimum yield force occurs at an absolute displacement (inter-story drift) of $\bar{u}_{fi} = \bar{u}_{ff} = 0.021$ for both stories.

Figure 5 presents the MLF solutions for several response quantities of the structure versus time for two different time step sizes; namely, 0.01 and 0.001. Notice that the results are nearly indistinguishable for these two analyses, except during the time step in which fracture occurred. The analysis results show that the first story fractured at approximately time 7.0 (Fig. 5b and 5c).

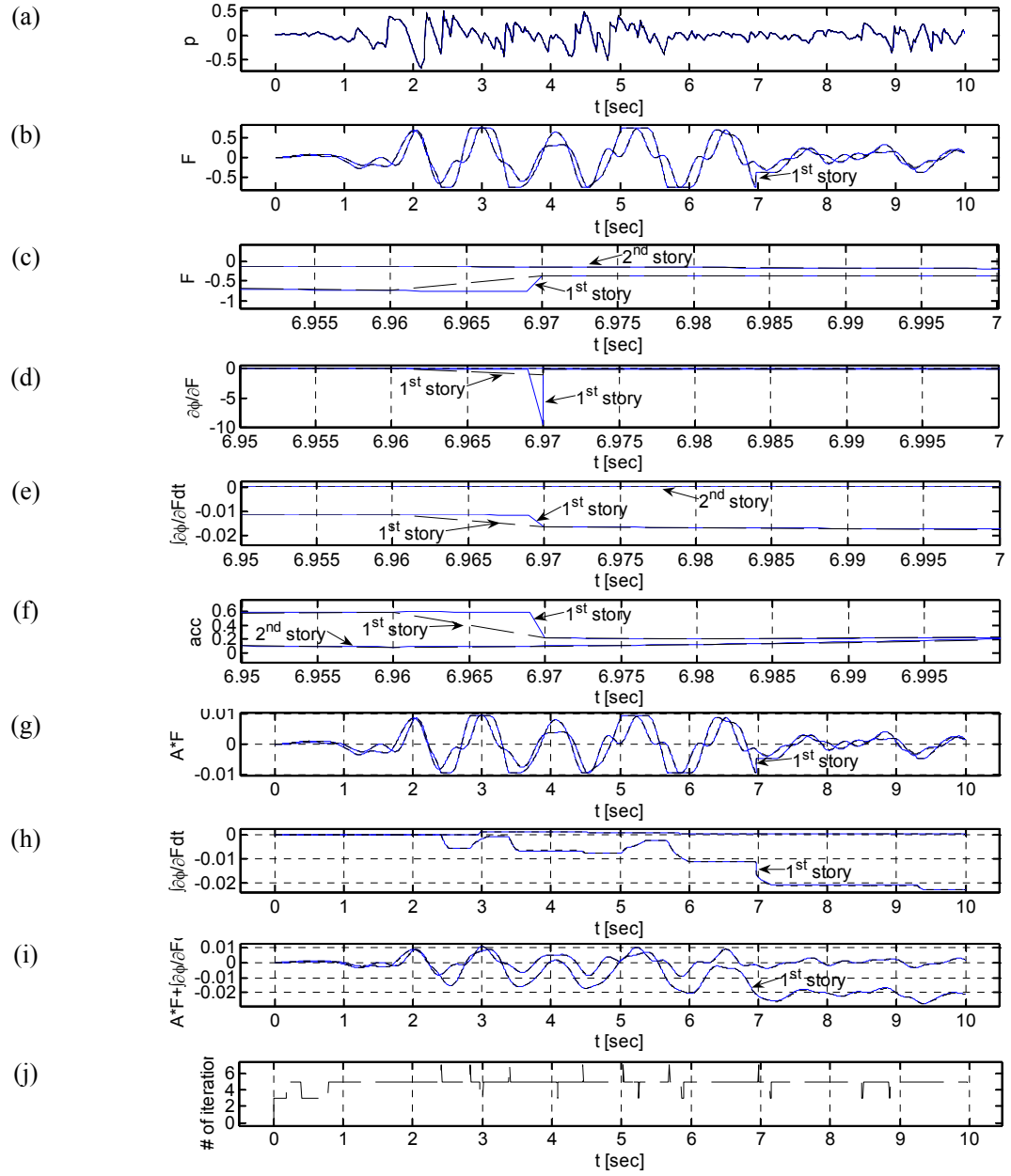

Figure 5 Response quantities versus time for 0.01 time step (dashed) and 0.001 time step (continuous); (a) External forces, (b) internal forces in the columns, (c) zoom on internal forces in the columns, (d) zoom on rate of plastic deformations, (e) zoom on plastic deformations, (f) zoom on accelerations of the masses, (g) elastic deformations, (h) rate of plastic deformations, (i) plastic deformations, (j) iteration counts.

Figures 5c-5f provide a zoom on the forces, rate of plastic deformations, plastic deformations and accelerations, respectively, near the time when fracture occurs. It can be seen that when sudden changes occur in some response quantities, they are "smeared" over a whole time step. Hence, with different time steps, a slightly different behavior is observed locally. However, when a step function is involved (see, for example, Fig. 5c, 5e and 5f), both solutions converge to the same values at the end of the longer time step. Moreover, when δ functions are involved (see, for example, Fig. 5d), the total area under these graphs, or their integral, is equal, as implied by Fig. 5e. Additional interesting observations are related to the physical behavior of the system. As expected, when fracture occurs, $\partial\varphi / \partial F$ shows a δ function with appropriate area of approximately $A \cdot \Delta F$ (Fig. 5c-5e). Moreover, the elastic deformation and plastic deformation show an equal and opposite "jump" of $A \cdot \Delta F$ (Fig. 5g and 5h), such that the sum of these deformations, which is actually the total deformation, remains a smooth function (Fig. 5i). In addition, the effect of the fracture of the first story on the acceleration of the first floor mass is clearly seen, where, as expected, this acceleration has a "jump" of $\Delta F/\mathrm{m}_i$ (Fig. 5f). In addition, the direct effect is seen on the acceleration of the first story only, as expected, since this force acts on the mass of the first floor only. From an algorithmic viewpoint, notice from Fig. 5j that the iteration counts for each time step are quite low, even for steps involving transitions to plasticity or for those encountering fracture.

6. CONCLUSIONS

In this paper a new unified fracture - strength degradation model using *strength reduction* rather than *negative stiffness* was developed. The consideration of strength degradation and fracture was done by modifying the MLF framework through "shrinking" of the yield surface. The derivations were developed for the general case of multi-dimensional plasticity. As shown, the structure of the optimization problem and solution of MLF is preserved with the addition of the new phenomena. This enables the use of the same optimization schemes through all stages of the analysis. The numerical scheme shows robustness, stability and convergence with relatively *large time steps sizes* even when fracture is considered, while still requiring only a *small number of iterations.* Insight to the behavior of the physical problem, as well as to the reason for the enhanced stability of the numerical scheme, was also presented. It was shown that the reason that MLF is so robust stems from the fact that the main variables used by MLF are *forces* and not displacements, and fracture is associated with *changing the constraints* on the forces rather than using a "negative stiffness". This actually leads to a constrained optimization problem that has a closed feasible region in each time step. Thus, the force vector cannot go beyond the plastic region and, consequently, the algorithm does not become unstable.

REFERENCES

Crisfield, M.A. (1991). Non-linear finite element analysis of solids and structures, John Wiley & Sons, Chichester, UK.

Reinhorn, A.M., Sivaselvan, M.V., Dargush, G.F. and Lavan O. (2007). Mixed Lagrangian formulation in analysis of collapse of structures, Computational methods in structural dynamics and earthquake engineering (COMPDYN2007), Rethymno, Crete, Greece.

Sivaselvan, M.V. and Reinhorn, A.M. (2000). Hysteretic models for deteriorating structures, *Journal of Engineering Mechanics, ASCE* **126**: 633-640.

Sivaselvan, M.V. and Reinhorn, A.M. (2006). Lagrangian approach to structural collapse simulation, *Journal of Engineering Mechanics, ASCE* **132**: 795-805.

Somerville, P., Smith, N., Punyamurthula, S. and Sun, J. (1997). Development of ground motion time histories for Phase 2 of the FEMA/SAC steel project. Report No. SAC/BD-97/04. (The ground motions can be downloaded from http://quiver.eerc.berkeley.edu:8080/studies/system/ground_motions.html.)